Log-periodic behavior of a hierarchical failure model with applications to precursory seismic activation

William I. Newman
Departments of Earth and Space Sciences, Physics and Astronomy, and Mathematics, University of California, Los Angeles, California 90095

Donald L. Turcotte
Department of Geological Sciences, Snee Hall, Cornell University, Ithaca, New York 14853

Andrei M. Gabrielov*
Mathematical Sciences Institute, Cornell University, Ithaca, New York 14853
(Received 15 May 1995)

Seismic activation has been recognized to occur before many major earthquakes, including the San Francisco Bay area prior to the 1906 earthquake. There is a serious concern that the recent series of earthquakes in Southern California is seismic activation prior to a great Southern California earthquake. The seismic activation prior to the Loma Prieta earthquake has been quantified in terms of a power-law increase in the regional Benioff strain release prior to this event and there is an excellent fit to a log-periodic increase in the Benioff strain release. In order to better understand activation a hierarchical seismic failure model has been studied. An array of stress-carrying elements is considered (formally, a cellular automaton or lattice gas, but analogous to the strands of an ideal, frictionless cable). Each element has a time to failure that is dependent on the stress the element carries and has a statistical distribution of values. When an element fails, the stress on the element is transferred to a neighboring element; if two adjacent elements fail, stress is transferred to two neighboring elements; if four elements fail, stress is transferred to four adjacent elements, and so forth. When stress is transferred to an element its time to failure is reduced. The intermediate size failure events prior to total failure each have a sequence of precursory failures, and these precursory failures each have an embedded precursory sequence of smaller failures. The total failure of the array appears to be a critical point. There is a sequence of partial failures leading up to the total failure that resembles a log-periodic sequence.

PACS number(s): 64.60.Ak, 64.60.Fr, 05.45.+b, 91.60.Ba

I. INTRODUCTION

Our present understanding of earthquakes is, at best, limited. There are two fundamental related problems that form the basis of the geomechanics of earthquakes and seismicity. The first of these concerns the mechanics of the faults on which earthquakes occur. How does the earthquake rupture initiate and how does it propagate? The second question concerns spatial correlations before earthquakes. The frequency-size distribution of earthquakes in a region is self-similar or "fractal" and earthquakes are accepted to be a type example of self-organization.

We first discuss the initiation and propagation of a rupture on a fault. The concept of a static coefficient of friction is generally applied to the initiation of rupture. Once the rupture initiates, a dynamic coefficient of friction is applied. Many solutions for this problem have been obtained assuming a single fault in a homogeneous stress field, i.e., Tse and Rice [1]. However, there are a number of serious problems with this approach. One major problem is the stress level. Observations (i.e., Zoback and Healy [2]) favor stress levels associated with failure on faults that are nearly an order of magnitude lower than the values predicted by laboratory friction experiments. This and other problems led Smalley *et al.* [3] to propose a hierarchical failure model for the initiation and propagation of failure on a fault. The asperities on a fault were treated as individual elements with a probabilistic distribution of strengths. If one element failed, the stress was transferred to the adjacent element on which an induced failure could occur. If two elements failed, the stresses were transferred to two adjacent elements and so forth. A cascade of failures occurred.

A universal feature of regional seismicity is that it satisfies the Gutenberg-Richter frequency-magnitude relation

$$\log_{10} N = a - bM_L \ , \tag{1.1}$$

with N the cumulative number of earthquakes with mag-

*Permanent address: Departments of Mathematics and Earth and Atmospheric Sciences, Purdue University, West Lafayette, IN 47907.

nitude greater than M_L and a and b constants. The dependence of N on M_L for Southern California for each year between 1980 and 1994 is given in Fig. 1. In general, there is good agreement with Eq. (1.1) taking $a = 4.3$ and $b = 1.06$. The exceptions can be attributed to the aftershock sequences of the Whittier (1987), Landers (1992), and Northridge (1994) earthquakes.

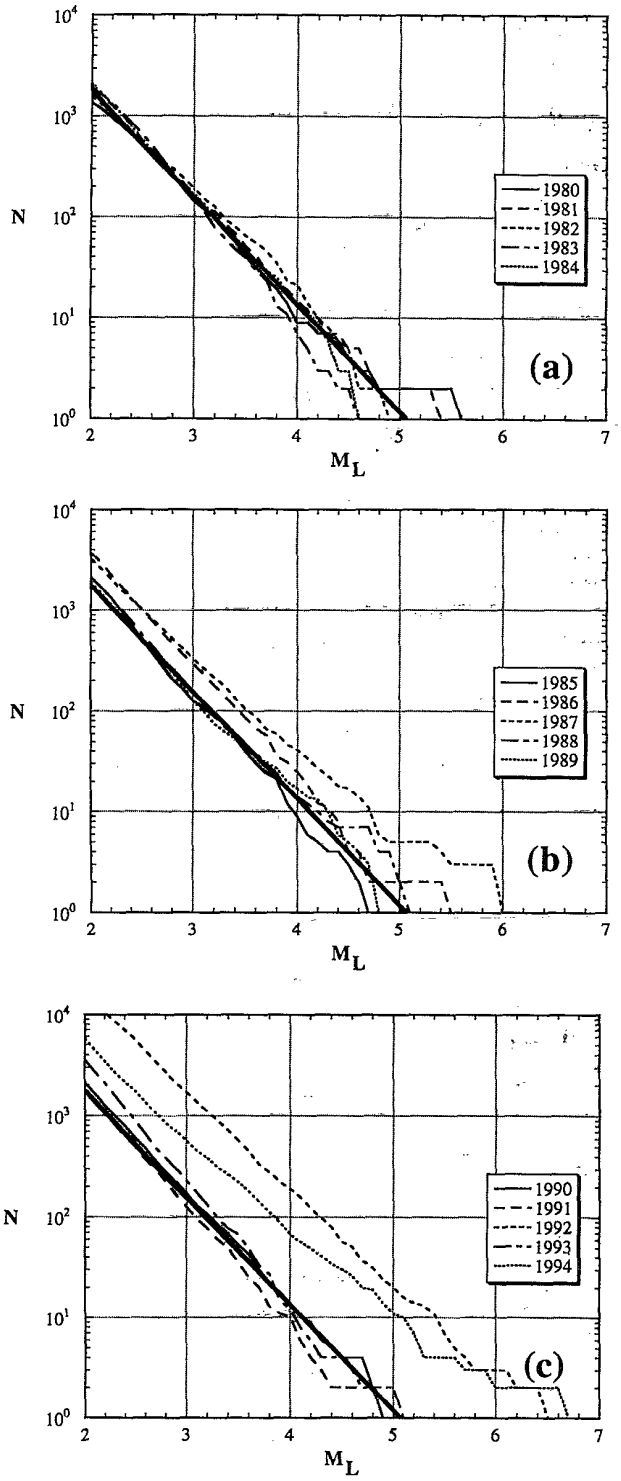

FIG. 1. The cumulative number of earthquakes N with magnitude greater than M_L for each year between 1980 and 1994 is given as a function of M_L, the region considered is Southern California. The straightline correlation is the Gutenberg-Richter relation (1.1) with $a = 4.3$ and $b = 1.06$.

The near uniformity of the background seismicity in Southern California is clearly striking. This is strongly suggestive of thermodynamic behavior and self-organization. There is increasing evidence that such long-distance correlations may be a characteristic of seismicity and are related to seismic activation.

Although long-distance correlations between earthquakes are a subject of considerable controversy, such correlations have been widely accepted in China and Russia (as well as the former Soviet Union). A striking example was a sequence of five earthquakes that occurred in China between 1966 and 1976. These were the $m = 7.2$ Shentai (1966), $m = 6.3$ Hijien (1967), $m = 7.4$ Bo Sea (1969), $m = 7.3$ Haicheng (1975), and the $m = 7.8$ Tangshan (1976). These earthquakes spanned a distance of some 700 km and the Haicheng earthquake was successfully predicted by the Chinese, at least partially on the basis of seismic activation [4].

Seismic activation has been previously recognized in association with an increase in seismicity that occurred in the San Francisco Bay area prior to the 1906 earthquake [5]. Earthquakes with estimated magnitudes between 6.5 and 7.0 occurred in 1865 (Santa Cruz Mountains), 1868 (Hayward), 1892 (Vacaville), and 1898 (Mare Island). There is a serious concern that a similar seismic activation is now underway in Southern California. A number of intermediate size earthquakes have occurred in Southern California in the last 45 years. These include the $m = 7.4$ Kern County earthquake on July 21, 1952, the $m = 6.4$ San Fernando earthquake on February 9, 1971, the $m = 7.6$ Landers earthquake on June 28, 1992, and the $m = 6.6$ Northridge earthquake on January 17, 1994.

Long-distance correlations and seismic activation form the basis of the pattern recognition earthquake prediction algorithms developed by a group of earthquake probabilists and statisticians in Moscow working under the direction of Vladimir Keilis-Borok. The pattern recognition included increases in regional seismicity, increases in the clustering of earthquakes, and changes in aftershock statistics. Premonitory seismicity patterns were found for strong earthquakes in California and Nevada (algorithm "CN") and for earthquakes with $M > 8$ worldwide (algorithm "M8"). Assuming self-similarity of the properties of seismicity, both algorithms were tested in seismically active regions [6]. When observed levels exceed preestablished thresholds, intermediate term (1–3 yr) predictions were made. TIP's (times of increased probability) were formally issued. During the last eight years, eight strong earthquakes (including Loma-Prieta, Landers, and Northridge) were predicted in advance.

This approach is certainly not without its critics. Independent studies have established the validity of the TIP for the Loma-Prieta earthquake; however, the occurrence of recognizable precursory patterns prior to the Landers earthquake are questionable. Also, the statistical significance of the size and time intervals of warnings in active seismic areas has been questioned. Nevertheless, seismic

activation prior to a major earthquake certainly appears to be one of the most promising approaches to earthquake prediction.

Seismic activation can be approached in a variety of ways. In one approach, the activation is attributed to an increase in the regional stress. As the stress is increased during a seismic cycle, there is a systematic increase in precursory activity before a major event occurs. This is essentially the approach that is modeled in this paper.

However, there is some indication that information is transmitted through the earth's crust in analogy to the transmission of information by collisions in a gas. The Landers earthquake showed that other earthquakes could be triggered at distances much greater than the rupture length of the earthquake [7].

The Landers earthquake provided direct evidence that faults interact with each other over large distances [7]. The Landers earthquake triggered earthquakes at 14 distant sites scattered over the western United States. The furthest site was Yellowstone National Park in Wyoming, 1250 km from Landers. The largest triggered earthquake, magnitude 5.6, occurred 250 km from Landers. Just how information is transmitted over these distances is uncertain. One hypothesis is that the surface waves of the Landers earthquake were responsible. The surface waves would be be equivalent to the thermal fluctuation involved in classical phase transitions.

Another approach to earthquake prediction based on long-distance correlations has been given by Sornette and Sammis [8]. This is an extension of an approach to earthquake prediction given by Varnes [9], Bufe and Varnes [10], and Bufe *et al.* [11]. These authors suggested that there was a power-law increase in the regional cumulative Benioff strain release prior to an earthquake. The data given by Bufe and Varnes [10] for the Loma Prieta earthquake is shown in Fig. 2. Sornette and Sammis [8] considered this data and concluded that there is an excellent fit to a log-periodic increase in seismic activity.

A simple power-law (fractal) increase in the cumulative Benioff strain E is given by

$$E = C(t_f - t)^{\alpha} , \tag{1.2}$$

where $t_f - t$ is the time prior to the earthquake and the constant α is negative. Bufe and Varnes [10] used this relation to predict the time t_f when the earthquake would occur. Consider the case when the exponent is complex: $\alpha = \xi + i\eta$. In this case Eq. (1.2) becomes

$$\begin{aligned} E &= \mathrm{Re}\{C(t_f - t)^{\xi + i\eta}\} \\ &= \mathrm{Re}\{Ct(t_f - t)^{\xi} \exp\{i\eta \ln(t_f - t)]\}\} \\ &= C(t_f - t)^{\xi} \cos\{\eta \ln(t_f - t)\} , \end{aligned} \tag{1.3}$$

where Re stands for the real part. This is log-periodic behavior. Results from condensed matter physics (see below) imply that additional terms with this increased complexity appear in the expression, supplementing the simple form in Eq. (1.2).

The possibility of complex scaling exponents and "log periodicity" in critical phenomena has been known for two decades [12]. Other work in areas of physics relevant to critical point phenomena and hierarchical structures shows how this could be an important influence. The subject of random walks on hierarchical or fractal structures, such as Sierpinski gaskets, has been intensively explored for nearly as long [13,14]. Magnetized systems, such as Ising models and spin glasses, have occupied a central role in considerations of critical phenomena and are capable of having complex exponents [15]. Chaotic spin glass models have been developed on fractal lattices [16] and, very recently, sandpile models built on Sierpinski gasket fractals [17] have been shown to exhibit a log-periodic oscillation. Of particular relevance to the present application, Blumenfeld and Ball [18] have found log-periodic behavior in their description of cracking.

The sequence of positive maxima in Eq. (1.3) corre-

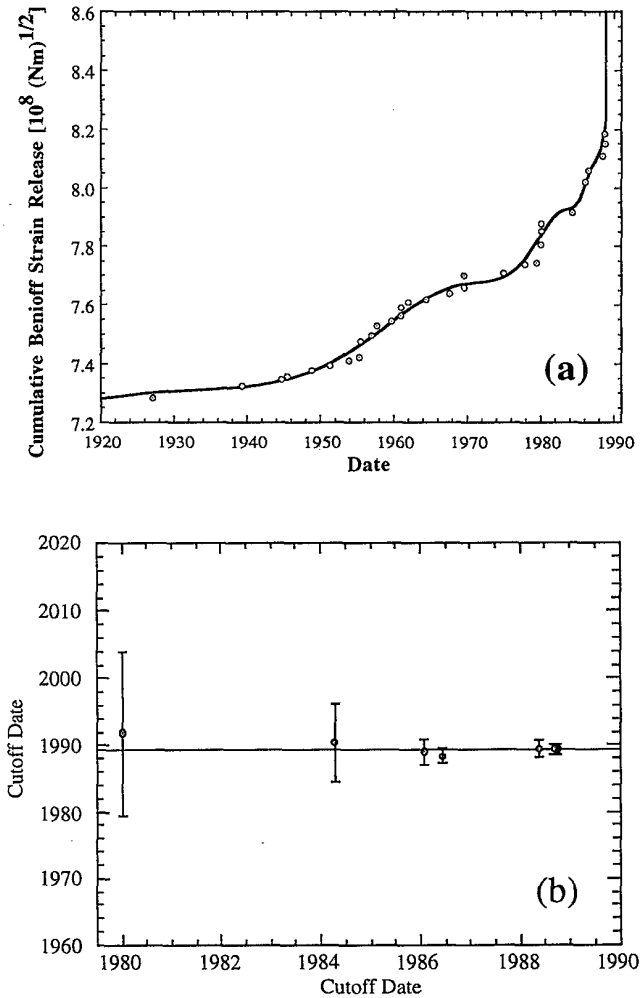

FIG. 2. (a) The data points are the cumulative Benioff strain release in magnitude 5 and greater earthquakes in the San Francisco Bay area prior to the October 17, 1989, Loma Prieta earthquake [10]. The solid line is the log-periodic correlation with the data. (b) Predicted dates for the Loma Prieta earthquake based on the data applicable prior to the cutoff date [8].

sponds to the sequence

$$t_f - t_n = \exp\left[\frac{1}{\eta}\tan^{-1}\left(\frac{\xi}{\eta}\right) + \frac{\pi n}{\eta}\right] \quad , \qquad (1.4)$$

where $n = 1, 2, 3, \ldots$. If three successive values of the maxima are observed, t_1, t_2, t_3, the failure time t_f is given by

$$t_f = \frac{t_2^2 - t_1 t_3}{2t_2 - t_1 - t_3} \quad . \qquad (1.5)$$

Thus, successive values of maxima can *in principle* be used directly to predict failure times.

Sornette and Sammis [8] introduced a more general form

$$E = A + B\,(t_f - t)^{\xi}\,\{1 + C\cos[\eta \ln(t_f - t) + \theta]\} \quad (1.6)$$

in keeping with a result in perturbation theory where additional terms like those in Eq. (1.3) must appear. The correlation of this result with the data of Bufe and Varnes [10] is illustrated in Fig. 2, and excellent agreement is found. This relation was used to obtain retrospective predictions for the occurrence of earthquakes and their predictions for the Loma Prieta earthquake are also illustrated in Fig. 2.

The concept of self-organized criticality (SOC) was introduced by Bak *et al.* [19]. SOC is defined to be a natural system in a marginally stable state that, when perturbed from that state, will evolve naturally back to the state of marginal stability. Energy input to the system is continuous but the energy loss is in a discrete set of events that satisfy self-similar or fractal frequency-size statistics. Distributed seismicity is taken to be the classic example of a natural system that exhibits self-organized criticality. There is a continuous input of energy (strain) through the relative motion of tectonic plates. This energy is dissipated in a fractal distribution of earthquakes, the Gutenberg-Richter relation Eq. (1.1) being equivalent to a fractal (power-law) relation between earthquake frequency and rupture area [20]. Scholz [21] has argued that the earth's entire crust is in a state of self-organized criticality. He makes the point that wherever a large dam is built induced seismicity results from the filling of the reservoir. Thus the crust is everywhere on the brink of failure. A variety of models that exhibit self-organized critical behavior (although the issue of "criticality" in these models remains somewhat controversial) yield similar statistics. One example is a two-dimensional array of slider blocks; the blocks are pulled over a surface by driver springs connected to a constant velocity driver plate, adjacent blocks are connected by connector springs. The blocks interact with the surface plate with a prescribed static-dynamic friction law. Many numerical studies of arrays have been carried out [22–28]. Fractal (i.e., self-similar [29]) frequency-size statistics of slip events are generally found. It is concluded that stress transfer between a hierarchical distribution of faults in the earth's crust is an essential feature of distributed seismicity.

In order to examine the questions discussed above, we consider a hierarchical, time-to-failure model for precursory activation. A series of elements is considered with each element having a prescribed lifetime. When elements fail, the stress on the elements is transferred to adjacent elements. This class of models has been applied to fibre bundles and composite materials [30–32]. We will show that this model incorporates many of the features of distributed seismicity and yields an activation prior to total failure that resembles a log-periodic sequence.

II. MODELS

Our hierarchical model for failure is illustrated in Fig. 3. It is a one-dimensional analog model for failure due to stress transfer. At the lowest order in this example, there are 128 zero-order elements. These elements are paired to give 64 first-order elements, the 64 first-order elements are paired to give 32 second-order elements, and so forth. A statistical distribution of lifetimes is assigned to the lowest-order elements. When one of these elements fails, the stress on the element is transferred to the neighboring element, increasing the stress on it. If a pair of zero-order elements fails, i.e., a first-order element, the stress is transferred to the adjacent pair of zero-order elements, i.e., to the adjacent first-order element, and so forth.

In order to illustrate the stress transfer, consider the second-order ($n = 4$) example given in Fig. 4. Each element is given a probabilistic "lifetime" and two examples of failure are illustrated. At time $t = 0$, the stress σ_0 is applied to the four elements. In both realizations element "2" has the shortest lifetime and it is the first to fail. The stress σ_0 on element "2" is transferred to element "1" placing a stress $2\sigma_0$ on this element as illustrated in Fig. 4(ii). The question now is whether the enhanced stress on element "1" will cause it to fail prior to elements "3" or "4." In realization 4(a), element "1" is the next to fail and the stress $2\sigma_0$ on this element is transferred to elements "3" and "4" placing a stress $2\sigma_0$ on both of these elements. Element "4" is the next to fail and the stress $2\sigma_0$ on it is transferred to the last surviving element "3," which has a stress $4\sigma_0$. In realization 4(b), element "4" is the next to fail and the stress σ_0 on this element is transferred to element "3" placing a stress $2\sigma_0$ on this element. Element "3" is the next to fail and the stress $2\sigma_0$ is again transferred to the last surviving

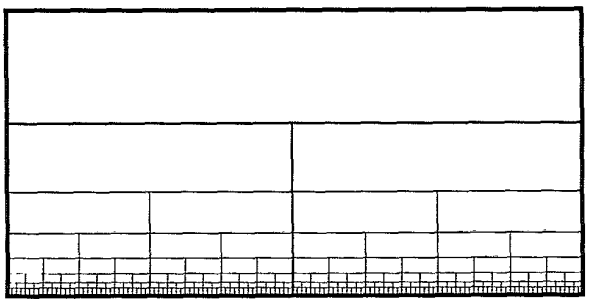

FIG. 3. Illustration of a seventh-order ($N = 128$) example of our hierarchical model.

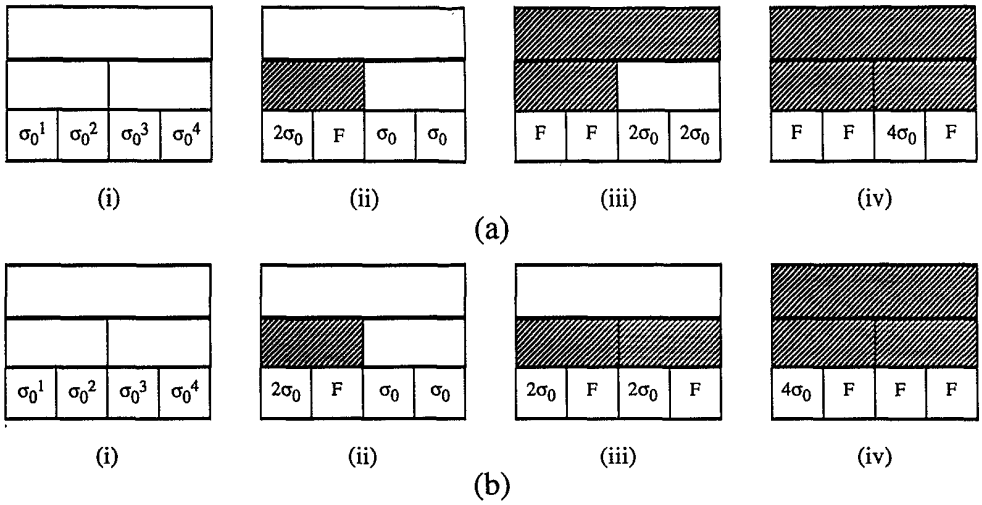

FIG. 4. Illustration of stress transfer in a second-order ($N = 4$) example of our hierarchical model. Each element is given a statistical "lifetime." In example (a), element "2" fails transferring stress to element "1," element "1" then fails and stress is transferred to elements "3" and "4," element "4" fails transferring stress to element 3 that subsequently fails. In example (b), element "2" fails transferring stress to element "1," element "4" fails transferring stress to element "3," element "3" fails transferring stress to element "1" that subsequently fails.

element "1", which has a stress $4\sigma_0$.

The zone of stress transfer is equal in size to the zone of failure. This local load sharing model simulates the Green's function associated with the elastic redistribution of stress adjacent to a rupture.

Before formulating the local load sharing model for failure, we will illustrate the approach by considering a simple global load sharing model. Initially we have N_0 elements each carrying a load σ_0. When an element fails, the load on that element is transferred uniformly to all the remaining elements—this is equivalent to a mean-field approximation. When n_f elements have failed, the stress σ on the $n_s = N_0 - n_f$ surviving elements is given by

$$\sigma = \frac{N_0}{N_0 - n_f}\sigma_0 \quad . \tag{2.1}$$

The rate at which elements fail is assumed to be given by the rate law

$$\frac{d(N_0 - n_f)}{dt} = -\nu(N_0 - n_f) \quad , \tag{2.2}$$

where the hazard rate ν is related to the stress by

$$\nu = \nu_0 \left(\frac{\sigma}{\sigma_0}\right)^{\rho} \quad , \tag{2.3}$$

where ν_0 is the hazard rate of a single element under load σ_0 and the power ρ is typically in the range of 2–5. Combining Eqs. (2.1) – (2.3) gives

$$\frac{d(N_0 - n_f)}{dt} = -\nu_0 \frac{N_0^{\rho}}{(N_0 - n_f)^{\rho - 1}} \quad . \tag{2.4}$$

Integrating with the condition that $n_f = N_O$ when $t = t_f$, we obtain

$$n_f(t) = N_0\{1 - [\rho\nu_0(t_f - t)]^{1/\rho}\} \quad . \tag{2.5}$$

The number of surviving elements has a power-law dependence on the time to failure with the exponent ρ^{-1}. This result is clearly similar to the power-law relation for increase in Benioff strain given in Eq. (1.2).

We now determine failure statistics for the hierarchical model illustrated in Fig. 3. Before obtaining numerical simulations, it is necessary to prescribe the failure statistics for the individual elements. The failure of an engineering material is generally modeled in terms of a statistical distribution of lifetimes when subject to an applied stress σ_0 [33,34]. The cumulative distribution of failure times t_f for an individual element can be written as

$$F(t_f) = 1 - \exp(-\nu_0 t_f) \quad , \tag{2.6}$$

where $\nu_0(\sigma_0)$ is the hazard rate under stress σ_0. This distribution of failure times is illustrated in Fig. 5, the mean lifetime of an element is $t_{1/2} = \nu_0^{-1} \ln 2$. Each of the N elements is assigned a failure time t_{i0} based on Eq. (2.6) for an applied stress σ_0. The statistical representation given in Eq. (2.6) is entirely equivalent to the failure statistics obtained from the rate law Eq. (2.2). Using the stress dependence introduced in Eq. (2.3), a Weibull distribution for failures is obtained

$$F(t_f) = 1 - \exp\left[-\nu_0 \left(\frac{\sigma}{\sigma_0}\right)^{\rho} t_f\right] \quad . \tag{2.7}$$

If elements are subjected to a constant stress σ at $t = 0$, Eq. (2.3) gives the statistical distribution of failure times t_f. The Weibull distribution is found to be in agreement with experiments on a wide variety of materials with ρ typically in the range $2 - 5$.

However, with stress transfer the stress is not neces-

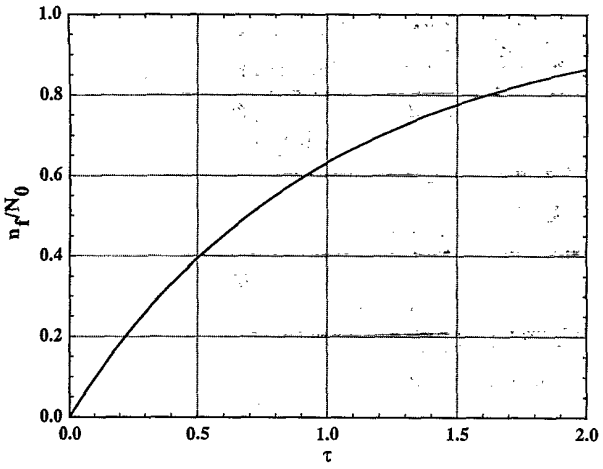

FIG. 5. Illustration of the cumulative distribution of nondimensional failure times $\nu_0 t_0$.

sarily constant. In order to accommodate the increase in stress caused by local load sharing from failed elements, we introduce a reduced time to failure for each element T_{if} for each element given by

$$t_{i0} = \int_0^{T_{if}} \left[\frac{\sigma(t)}{\sigma_0}\right]^{\rho} dt \ . \tag{2.8}$$

Each element i is assigned a random time to failure t_{i0} under stress σ_0 based on Eq. (2.6). The actual time to failure of element i, namely T_{if}, is reduced below t_{i0} if stress is transferred to the element. The time T_{if} is obtained by requiring that Eq. (2.8) is satisfied.

Consider the example illustrated in Fig. 4(a). The four elements $i = 1, 2, 3, 4$ carrying stress σ_0 are assigned failure times t_{10}, t_{20}, t_{30}, and t_{40} using the probability distribution Eq. (2.8). Element "2" has the shortest failure time so that

$$T_{2f} = t_{20} \ . \tag{2.9}$$

Upon failure the stress σ_0 carried by this element is transferred to element "1" as illustrated in Fig. 4(a ii). Element "1" is the next element to fail and its failure time T_{1f} is given by

$$T_{1f} = t_{20}\left(1 - 2^{-\rho}\right) + 2^{-\rho} t_{10} \ . \tag{2.10}$$

Upon the failure of "1", the stress $2\sigma_0$ is transferred to elements "3" and "4" as illustrated in Fig. 4(a iii). Element "4" is the next element to fail and its failure time T_{4f} is given by

$$\begin{aligned} T_{4f} &= T_{1f}\left(1 - 2^{-\rho}\right) + 2^{-\rho} t_{40} \\ &= t_{20}\left(1 - 2^{-\rho}\right)^2 + t_{10}\left(1 - 2^{-\rho}\right) 2^{-\rho} + 2^{-\rho} t_{40} \ . \end{aligned} \tag{2.11}$$

Upon the failure of "4," the stress σ_0 is transferred to element "3" as illustrated in Fig. 4(a iv). The time to failure of element "3" is given by

$$\begin{aligned} T_{3f} = t_{20}\left(1 - 2^{-\rho}\right)^2 + (t_{10} + t_{40})\left(1 - 2^{-\rho}\right) 2^{-\rho} \\ + t_{30} 2^{-2\rho} \ . \end{aligned} \tag{2.12}$$

Alternative failure sequences are also possible, one example is illustrated in Fig. 4(b). Again "2" is the first element to fail, however in this case the second element to fail is "4," then "3" fails and finally "1" fails. Newman *et al.* [32] provide computationally optimal methods for performing the lifetime calculations for large arrays of elements and provide numerical evidence for the existence of a critical point.

III. RESULTS

We have carried out a sequence of numerical experiments using 12th-order (N=4096) and 16th-order (N = 65 536) realizations of our model with $\rho = 4$. An example of a 16th-order realization is given in Fig. 6. The total failure sequence is given in Fig. 6(a). The nondimensional time is taken to be $\tau = \nu_0 t$ and failure in the case occurs at $\tau = 0.048\,027$. It is interesting that failure occurs at a nondimensional time, which is more than an order of magnitude *shorter* than the mean time to failure of an individual element $\tau_{1/2} = 0.613\,15$. The lifetime of our composite material is much shorter than the mean lifetime of individual elements. This observation may help to explain why actual faults are much weaker than predictions based on laboratory friction experiments. Failure stresses on faults are about one order of magnitude lower than values obtained by extrapolations of the laboratory studies. This is known as the "heat flow paradox" since the expected frictional heating on faults is not observed [35].

The failure sequence between $\tau = 0.0445$ and failure is expanded in Fig. 6(b). There is a well-defined sequence of partial failures prior to the total failure at $\tau_f = 0.048\,027$. Well-defined partial failures occur at $\tau_1 = 0.047\,965$, $\tau_2 = 0.047\,799$, $\tau_3 = 0.047\,487$, $\tau_4 = 0.047\,162$, and $\tau_5 = 0.046\,124$. The failure sequence between $\tau = 0.047\,45$ and $\tau = 0.047\,85$ is further expanded in Fig. 6(c) to show the structure of the partial failures at $\tau = 0.047\,799\,2$ and $\tau = 0.047\,487$. In each case there is a nested sequence of higher-order partial failures. Further expansion would show higher orders of nesting. The structure is basically self-similar or fractal. There is a scale invariant sequence of precursory failures at all levels. Because of the stochastic nature of the model the embedding is not always clear, a particular partial failure may be part of a sequence or may be precursory to another failure in the sequence. But this is also the problem with distributed seismicity.

It is also of interest to determine whether the sequence of partial failures can be inserted into the predictive log-periodic relation Eq. (1.5) in order to predict the time of the total failure. Taking the sequence of partial failures τ_5, τ_4, and τ_3, we obtain the prediction $\tau_f = 0.047\,636\,48$ from Eq. (1.5); taking the sequence τ_4, τ_3, and τ_2, we obtain $\tau_f = 0.054\,774\,75$ from Eq. (1.5); and taking the sequence τ_3, τ_2, and τ_1, we obtain $\tau_f = 0.048\,153\,62$ from

Eq. (1.5). These results are summarized in Table I. There is clearly considerable scatter in the predictions. Other realizations give similar results. Although the embedded sequences of precursory failures are a ubiquitous feature of all realizations, there is considerable stochastic variability of the timing. This is also a characteristic feature of distributed seismicity.

In Fig. 7, the logarithm of the number of unfailed elements is given as a function of the logarithm of the time to failure for a realization with 4096 points and $\rho = 4$. The power-law fit shown by the dashed line has a slope of 0.24, this compares with the power $\rho = 0.25$ predicted by the global load sharing relation Eq. (2.7). Although there is considerable scatter, the power-law relation does appear to be a reasonable predictor for our model just as Bufe and Varnes [10] found for regional seismicity. It is important to note, however, that the quality of the fit deteriorates as complete failure is approached. The global analysis employed in the derivation of Eq. (2.7) deteriorates owing to the increasing importance of localization in the evolution of the cascade of failures.

The sequence of failures as a function of position on

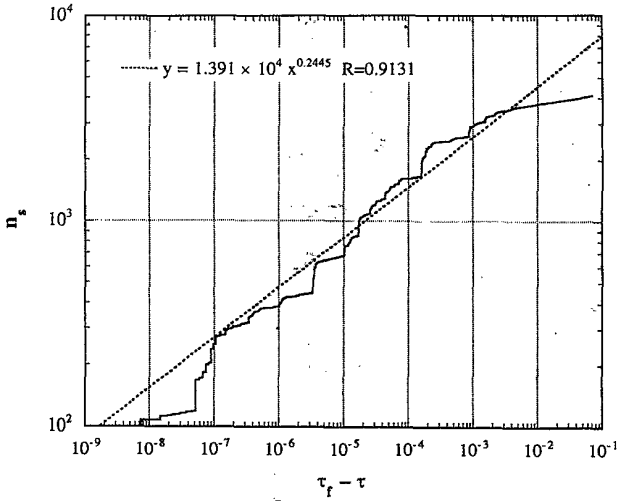

FIG. 7. Failure sequence for a 12th-order ($N = 4096$) realization of our model. The dashed line is a power-law fit to the failure sequence based on Eq. (1.5).

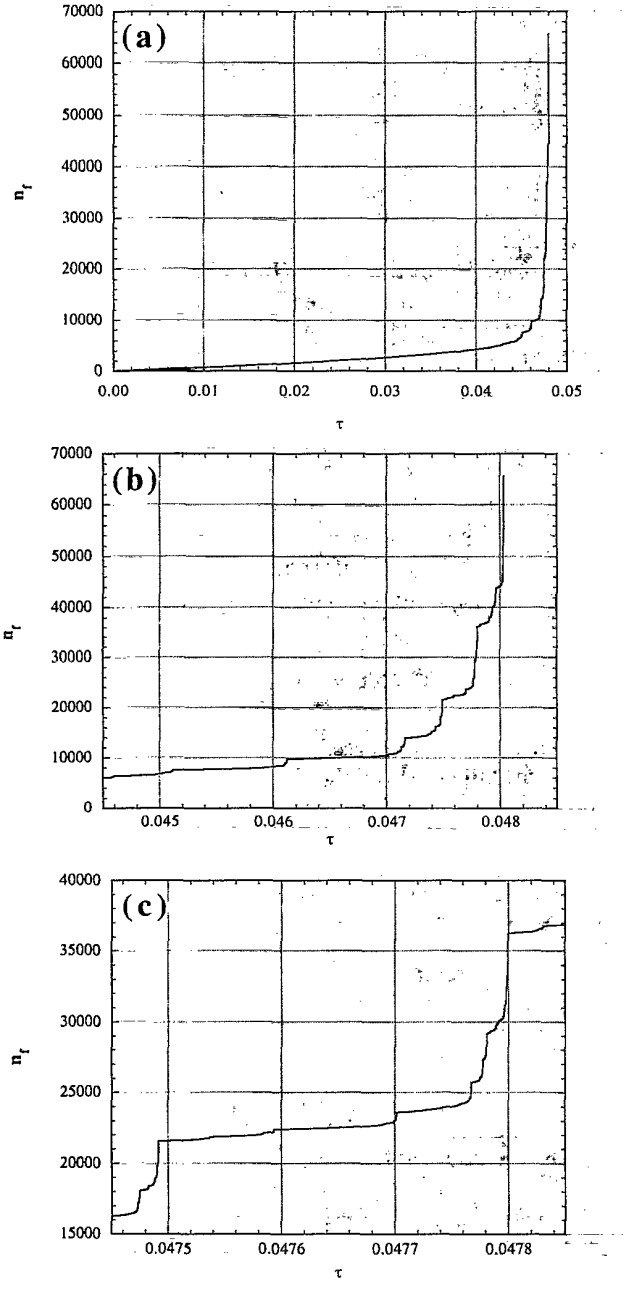

FIG. 6. Failure sequence for a 16th-order ($N = 65\,536$) realization of our model. (a) Entire failure sequence (failure is completed at $\tau = 0.048\,026\,6$). (b) Expansion of the final sequence of partial failures. (c) Further expansion of two partial failures.

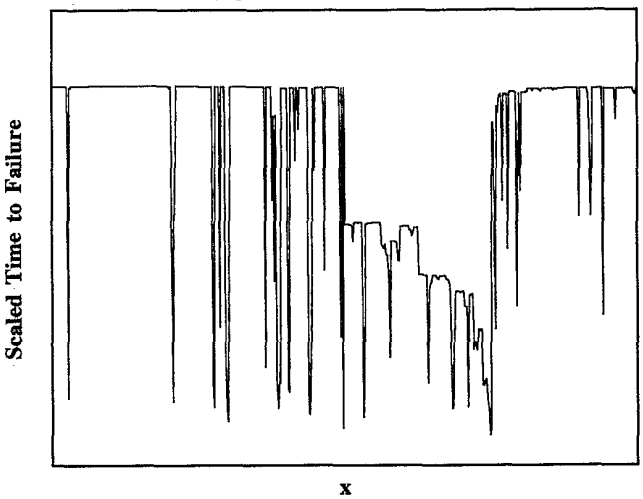

FIG. 8. Sequence of failures as a function of position. First 512 elements.

TABLE I. Realization of failure using 65 536 point simulation. Three successive "events" were employed to "predict" total failure. Three sets of successive events were considered to provide estimate of error. True failure time is also given.

0.046 125 0.047 162 0.047 487	⇒	0.047 636, 1st est.	⇒	0.048 627, true failure time
0.047 162 0.047 487 0.047 799	⇒	0.054 775, 2nd est.		
0.047 487 0.047 799 0.047 965	⇒	0.048 154, 3rd est.		

the linear array of elements is shown in Fig. 8(a) for the above realization. An expanded version for the first 512 points is shown in Fig. 8(b). The precursory cascades of failure are clearly illustrated. This figure illustrates the growing importance of localization in failure events as criticality is approached. We will explore and analyze the behavior of the cascade when failure is imminent in a future paper.

IV. CONCLUSIONS

We have explored by computational means the behavior of a hierarchical model for failure in time of a material. This hierarchical description accommodates the redistribution of stress from failed portions of a material to nearest regions of comparable size and provides a probabilistic realization of the accelerating tendency of material whose load has increased substantially to fail. This model also manifests some of the self-similar or "fractal" scaling features that are now recognized as being associated with seismicity and faulting. When a mean-field approximation is applied, a power-law distribution of failures is found prior to total failure. With the hierarchical model, a log-periodic distribution of failure is found prior to total failure. (In condensed matter applications, this is usually the signature of discreteness on the smallest scale [12].) A log-periodic increase in the regional Benioff strain was observed prior to the Loma Prieta earthquake. Although the detailed association of our model with precursory seismicity remains to be defined clearly,we consider this model to be a representation for seismic activation and find failure properties similar to those observed prior to large earthquakes. We plan to explore in future work the significance of the events occurring just before failure and their potential value in predicting great earthquakes.

ACKNOWLEDGMENTS

A.M.G. was supported in part by the U.S. Army Research Office through the Army Center of Excellence for Symbolic Methods in Algorithmic Mathematics (ACSyAM), Mathematical Sciences Institute of Cornell University, Contract No. DAAL03-91-C-0027. A.M.G. and D.L.T. have been partially supported under NSF Grant No. EAR942-3818.

[1] S.T. Tse and J.R. Rice, J. Geophys. Res. **91**, 9452 (1986).
[2] M.D. Zoback and J.H. Healy, J. Geophys. Res. **97**, 5039 (1992).
[3] R.F. Smalley, D.L. Turcotte, and S.A. Solla, J. Geophys. Res. **90**, 1894 (1985).
[4] C.H. Scholz, Nature **267**, 121 (1977).
[5] L.R. Sykes and S.C. Jaume, Nature **348**, 595 (1990).
[6] V.I. Keilis-Borok, Rev. Geophys. **28**, 19 (1990).
[7] D.P. Hill, P.A. Reasenberg, A. Michael, W.J. Arabaz, G. Beroza, D. Brumbaugh, J.N. Brune, R. Castro, S. Davis, D. dePolo, W.L. Ellsworth, J. Gomberg, S. Harmsen, L. House, S.M. Jackson, M.J.S. Johnston, L. Jones, R. Keller, S. Malone, L. Munguia, S. Nava, J.C. Pechmann, A. Sanford, R.W. Simpson, R.B. Smith, M. Stark, M. Stickney, A. Vidal, S. Walter, V. Wong, and J. Zollweg, Science **260**, 1617 (1993).
[8] D. Sornette and C.G. Sammis, J. Phys. (France) I **5**, 607 (1995).
[9] D.J. Varnes, Pure Appl. Geophys. **130**, 661 (1989).
[10] C.G. Bufe and D.J. Varnes, J. Geophys. Res. **98**, 9871 (1993).
[11] C.G. Bufe, S.P. Nishenko, and D.J. Varnes, Pure Appl. Geophys. **142**, 83 (1994).
[12] M. Nauenberg, J. Phys. A **8**, 925 (1975).
[13] M. Schreckenberg, Z. Phys. B **60**, 483 (1985).
[14] B. O'Shaughnessy and I. Procaccia, Phys. Rev. A **32**,

3073 (1985).
[15] J.-H. Chen and T.C. Lubensky, Phys. Rev. B **16**, 2106 (1977).
[16] A.N. Berker and S.R. McKay, J. Stat. Phys. **36**, 787 (1984).
[17] B. Kutjnak-Urbanc, S. Zapperi, S. Milošević, and H.E. Stanley (unpublished).
[18] R. Blumenfeld and R.C. Ball, Physica A **177**, 407 (1991).
[19] P. Bak, C. Tang, and K. Wiesenfeld, Phys. Rev. A **38**, 364 (1988).
[20] K. Aki, in *Earthquake Prediction*, edited by D.W. Simpson and P.G. Richards (American Geophysical Union, Washington, DC, 1981), pp. 566–574.
[21] C.H. Scholz, in *Spontaneous Formation of Space-time Structures and Criticality*, edited by T. Riste and D. Sherrington (Kluwer Academic Publishers, Netherlands, 1991), pp. 41–56.
[22] J.M. Carlson and J.S. Langer, Phys. Rev. A **40**, 6470 (1989).
[23] J.M. Carlson, J.S. Langer, B.E. Shaw, and C. Tang, Phys. Rev. A **44**, 884 (1991).
[24] H. Nakanishi, Phys. Rev. A **41**, 7086 (1990).
[25] H. Nakanishi, Phys. Rev. A **43**, 6613 (1991).
[26] S.R. Brown, C.H. Scholz, and J.B. Rundle, Geophys. Res. Lett. **18**, 215 (1991).
[27] K. Ito and M. Matsuzaki, J. Geophys. Res. **95**, 6853 (1990).
[28] J. Huang, G. Narkounskaia, and D.L. Turcotte, Geophys. J. Int. **111**, 259 (1992).
[29] D.L. Turcotte, *Fractals and Chaos in Geology and Geophysics* (Cambridge University Press, Cambridge, 1992).
[30] S.L. Phoenix and L.J. Tierney, Eng. Fract. Mech. **18**, 193 (1983).
[31] W.I. Newman and A.M. Gabrielov, Int. J. Fract. **50**, 1 (1991).
[32] W.I. Newman, A.M. Gabrielov, T.A. Durand, S.L. Phoenix, and D.L. Turcotte, Physica D **77**, 200 (1994).
[33] B.D. Coleman, Trans. Soc. Rheol. **1**, 153 (1957).
[34] B.D. Coleman, J. Appl. Phys. **29**, 968 (1958).
[35] A.H. Lachenbruch and J.H. Sass, J. Geophys. Res. **97**, 4995 (1992).